



STEEPNESS OF THE LATERAL DISTRIBUTION FUNCTION OF SECONDARY HADRONS IN EXTENSIVE AIR SHOWERS

M. Roshan Nasab

Physics Department, University of Semnan, Semnan, Iran

G. Rastegarzadeh

Physics Department, University of Semnan, Semnan, Iran

ABSTRACT

The influence of high and low energy hadronic interaction models on hadrons lateral distribution of cosmic ray air showers for primary energies 10^{17} - 10^{19} eV is explored. By using CORSIKA simulation code hadrons lateral distribution and also steepness of the hadron lateral distribution function is studied. We have shown η (the steepness of the lateral distribution) is increases with increasing primary energy and is decreases with increasing primary mass. We have investigated hadrons lateral distribution and their dependence on the primary energy and mass of cosmic ray induced air showers. η can be directly related to the shower maximum (X_{max}) and also it can suitable parameters for resolution of composition mass of cosmic ray.

© 2014 AESS Publications. All Rights Reserved.

Keywords: Cosmic ray, Extensive air shower, Secondary hadrons, The steepness of lateral distribution function, Lateral distribution, CORSIKA, QGSJET and DPMJET models.

1. INTRODUCTION

The interaction of high energy cosmic ray particles with the atmospheric nuclei creates an (EAS) which contains secondary particles like electrons, muons and hadrons. The interpretation of extensive air shower (EAS) measurements depends on the comparison with EAS simulations. Direct measurements of the primary cosmic rays (CR) with energies $\geq 10^{12}$ eV are generally difficult due to their exceedingly low flux. Instead, their properties are reconstructed from the shape and particle content of the extensive air showers (EAS) they produce in the atmosphere. The reconstruction is based on numerical models of the air shower development.

Hadrons constitute the least abundant particle group in air showers. They contribute about % 1 to the total particle flux but are chiefly responsible for the energy transport and supply in the shower process. They are sensitive to hadronic interaction models which have to extrapolate into kinematical and energy regions not covered by present-day collider experiments. Therefore, they can be used to check the reliability of the interaction models.

The measurement of secondary parameters such as lateral density distribution carries important information about the shower development and type of primary. The determination of the lateral density distribution of hadrons in showers is of important when studying propagation, interaction and energy flow of the hadronic component is investigated. Study of the width of hadron lateral distributions (HLD) can give data on the change in the transverse momentum P_t in interactions with air nuclei with an increase in the energy E_0 . Up to now different functions for shape of lateral distribution have been used. Lateral distribution of electrons with correlation of NKG [1, 2] and lateral distribution of muon by function of Greisen [2, 3] are examined. The best expression to describe the lateral density distribution of hadrons in air showers is given by [4]

$$\rho_h(E_h, r) = N_h(> E_T) f_h(r) \quad (1)$$

Where $N_h(>E_T)$ is the total number of hadrons with energy $>E_T$, and $f_h(r)$ is the characteristic function of the lateral distribution of the hadrons and is given by

$$f_h(r) = \frac{1}{8! \pi r_0^2} \left[\left(-\frac{r}{r_0} \right)^{0.25} \right] \quad (2)$$

In the present work we focus on hadronic component of extensive air shower to investigate hadrons lateral distribution and η (the steepness of hadrons lateral distribution) at the different energy and mass of primary. The shower simulations are performed using CORSIKA-7/400 code [5] with thinning [6] method and hadronic interactions are modeled using the GHEISHA [5, 7] code at low energies ($E < 80$ GeV). Moreover, the DPMJET [5, 8] and the QGSJET [5, 9] are utilized as high energy interactions. Vertical showers initiated by primary protons and iron nuclei are simulated. Observation level is taken at the 110m. Standard atmosphere and default magnetic field in CORSIKA are taken. 300 showers are simulated each for rang of primary energies 10^{17} - 10^{19} eV. All together 1200 showers are generated.

The paper is arranged as follows. Section 2 provides Hadrons lateral distribution. Section 3 deals with the steepness of lateral distribution of hadrons η in different primary mass, energies and DPMJET, QGSJET models.

2. HADRONS LATERAL DISTRIBUTION

Lateral distribution of hadrons in EAS is of interest because by integrating the lateral distribution the total number, the average radius of hadrons and the total energy flow by hadrons in EAS can obtained and also that study of lateral distribution can provide us with the information about the mean value of the transvers momentum in high energy interactions. Energetic secondary hadrons have transverse momenta that are very small compared to their longitudinal momenta. They travel close to the shower axis and essentially parallel to it.

Multiple scattering of electrons resembles the scattering characters of hadrons with of mean transvers momentum of 400MeV/c almost irrespective of their energy. Hence, in a dimensional estimate of the hadonic lateral scale radius we substitute in the formula of the Moliere radius

$$R_M = X_0 \times \frac{E_s}{E_c} \quad \text{the radiation length } X_0 \text{ by the hadronic interaction length, the scaling energy}$$

$$E_s = m_e c^2 \sqrt{4\pi/\alpha} \cong 21.2 \text{MeV by the mean transverse momentum and, the critical energy } E_c \text{ by}$$

Threshold energy detected hadrons and, arrive at radius of core distance $r_h \cong 1.2\text{km}400\text{MeV}/50\text{GeV} \cong 10\text{m}$ [2] such as observed in following figures.

Figure 1: Shows lateral distribution of secondary hadrons to the primary beams of proton and iron at primary energy 10^{17} eV are simulated. As is evident within distance of 10 meters of the shower core density hadrons have dropped sharply. Also lateral density of secondary hadrons to the proton primary is more than iron primary. Duo to secondary hadrons of initial proton energy per nucleons is more and greater depth of shower maximum X_{max} consequently has been more lateral distribution. Comparison of hadrons density for primaries proton and iron at primary energy 10^{19} eV are shown in Figure 2. Due to figure1 hadrons density is more in this figure and hadrons of primary proton and iron are almost overlapping.

The influence of high energy interaction models QGSJET, DPMJET on the lateral distribution of secondary hadrons for proton initial at primary energy 10^{19} eV are shown in Figure 3. Model QGSJET, density of hadrons at shower core greater is predicted. At greater distances from the shower axis is less difference between the models. Since at high energies the uncertainty be greater, In distance from the shower axis due to decrease of energy is lower models uncertainty. Models difference in the prediction of secondary hadrons of iron is order to protons differences that are shown in Figure 4.

3. THE STEEPNESS OF LATERAL DISTRIBUTION OF HADRONS η

In the present work the results of simulations of the lateral density of hadrons are fitted with the equation (3). In this equation, $\rho_h(r)$ hadrons density at distance r from the shower axis and k , η and r_0 are fitting parameters.

$$\rho_h(r) = kr^{-(\eta+\frac{r}{r_0})} \quad \text{Ave, et al. [10]} \quad (3)$$

Parameter η is the steepness of the distribution function of lateral hadrons. Dependence of η to maximum depth of the shower X_{max} directly is specified. Whatever X_{max} is closer to the level observation (primary mass of less and primary energy of more) lateral distribution will be sharper (η more). Therefore the steepness of hadrons lateral distribution a sensitive parameter to mass and energy will be.

Density of secondary hadrons for the initial protons at energy 10^{19} eV with the fitted curve with the equation (3) is shown in Figure 5. Parameter of r_0 in this Figure $r_0 = 30\text{m}$ has been selected that of order lateral distribution of hadrons $r_h = 10\text{m}$. The simulation fitted very well with equation (3) shows ($R^2=99\%$).

The steepness of lateral distribution of hadrons for primary protons and iron as a function of primary energy by models QGSJET and DPMjet are shown in Figures 6 and 7. For both iron and proton the mass is high η to increase energy. In addition, the steepness of the lateral distribution of hadrons for protons is more than iron. In each of case the increase of η due to is increasing depth of maximum X_{max} .

For investigate the effect of hadronic interaction models on the value η , Dependence η on the primary energy for primary iron by models QGSJET and DPMjet is shown in Figure 8 and also for primary proton shown in Figure 9. The model QGSJET predicts greater values for η . As can be observed the difference between models for the iron primary mass in lower primary energy is lower

because in the low primary energy, the energy per nucleons in nuclei of iron is lower than protons. As a result, impact of uncertainty of models at the low energies is less.

4. CONCLUSIONS

Dependence of the steepness of lateral distribution η of hadrons to primary of mass and energy is studied. We show that by increasing the primary energy η is increased and with increasing primary mass is reduced, therefore it can suitable parameters for resolution of composition mass of cosmic ray. Difference between high-energy hadronic interaction models QGSJET and DPMjet in anticipation of the steepness of lateral distribution of hadrons η is investigated. We show that the greater values of η for model QGSJET at compared with model DPMjet is predicted. Due to predictions QGSJET and DPMJET high energy interaction models, it is found that QGSJET model results high values of η with respect to DPMJET model, hence lighter mass composition.

REFERENCES

- [1] K. Dipsikha and K. Boruah, "Study of lateral distribution parameters from simulation of HE cosmic ray EAS," presented at the 32nd International Cosmic Ray Conference, Beijing, 2011.
- [2] T. Antoni and W. D. Apel, "Electron, muon, and hadron lateral distributions measured in air showers by the KASCADE experiment," *Astroparticle Physics*, vol. 14, pp. 245-260, 2001.
- [3] G. Hovsepyan, A. Chilingarian, G. Gharagozyan, S. Ghazaryan, E. Mamijanyan, and L. Melkumyan, "The lateral distribution function of extensive air showers measured by maket-ANI detector," presented at the 29th International Cosmic Ray Conference, 2005.
- [4] K. F. Peter, "Greider extensive air shower," *Springer Science*, vol. 1, pp. 685-700, 2010.
- [5] D. Heck, J. Knapp, J. Capdevielle, G. Schatz, and T. Thouw, "CORSIKA: Amonte carlo code to simulate extinsive air shower wissens chaftliche berichte," *Forschungszentrum Karlsruhe FZKA, p6019*, vol. 1, pp. 1-169, 1998.
- [6] B. T. Stokesa, R. Cady, D. Ivanova, J. N. Matthews, and G. B. Thomson, "Dethinning extensive air shower simulations [astro-ph.IM], 1104.3182," vol. 3, pp. 625- 29 2012.
- [7] W. D. Apel and A. F. Badea1, "Test of interaction models up to 40 PeV by studying hadronic cores of EAS," *Journal of Physics G: Nuclear and Particle Physics*, vol. 34, pp. 2581-2593, 2007.
- [8] J. Milke and J. R. Hoerandel, "Test of hadronic interaction models with KASCADE," *Acta Physica Polonica B.*, vol. 35, pp. 341-349, 2005.
- [9] D. Heck and R. Engel1, "Influence of low energy hadronic interaction program ones air shower simulations with CORSIKA," presented at the 28th International Cosmic Ray Conference, 2003.
- [10] M. Ave, O. L. Caz, J. A. Hinton, J. Knapp, J. Lloyd-Evans, and A. A. Watson, "Mass composition of cosmic rays in the range $2 \times 10^{17} - 3 \times 10^{18}$ eV measured with the Haverah park Array Astro-ph /0203150," vol. 1, pp. 1140-156, 2002.

Figure-1. Prediction models QGSJET form lateral distribution of secondary hadrons with primary of proton and iron at 10^{17} eV.

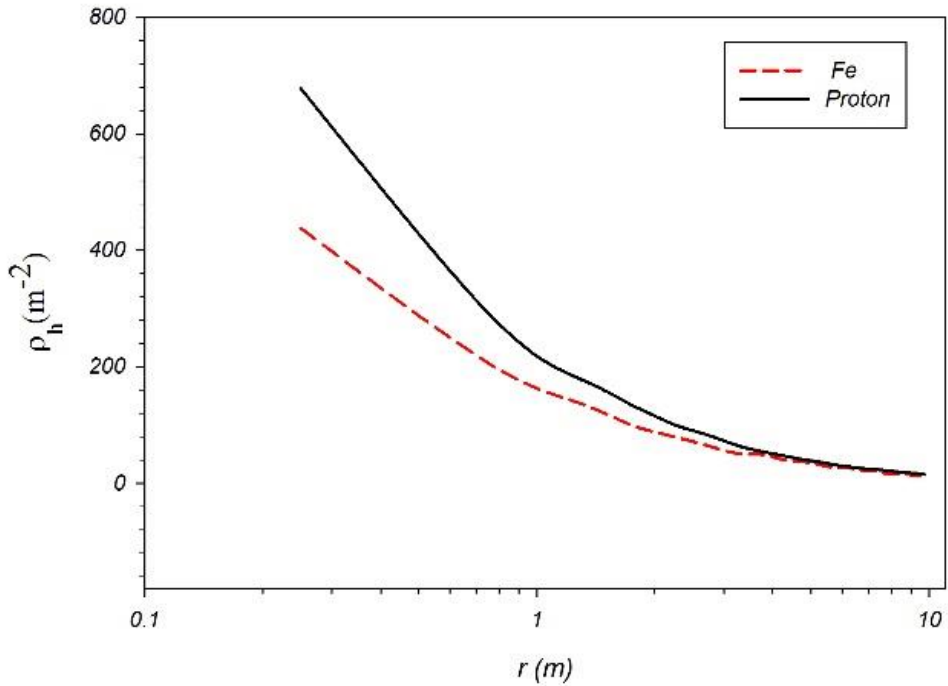


Figure-2. Prediction DPMJET model form lateral distribution of secondary hadrons with primary of proton and iron at 10^{19} eV.

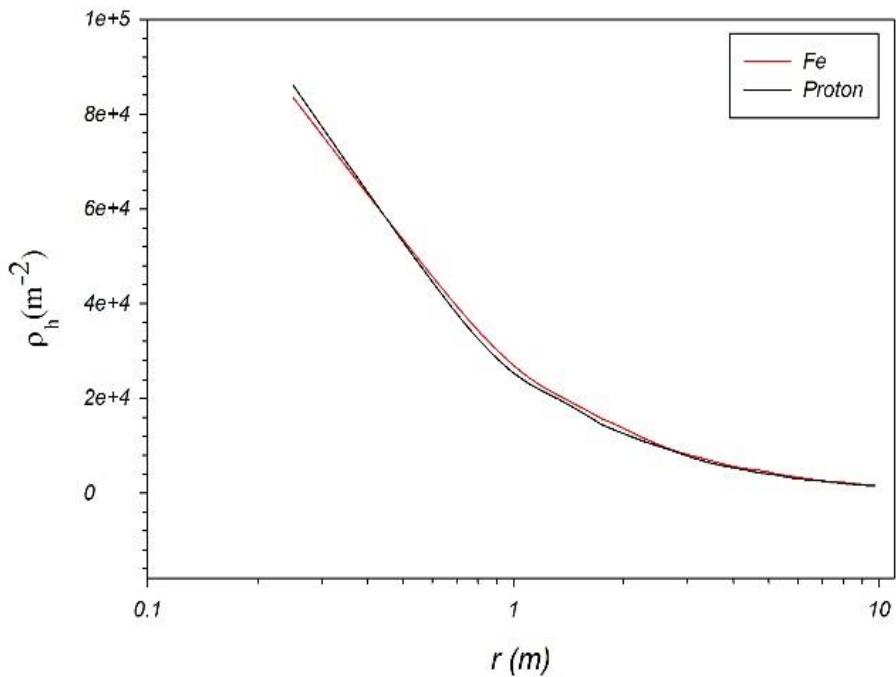


Figure-3. Prediction QGSJET, DPMJET models of lateral distribution of secondary hadrons with primary iron at 10^{19} eV.

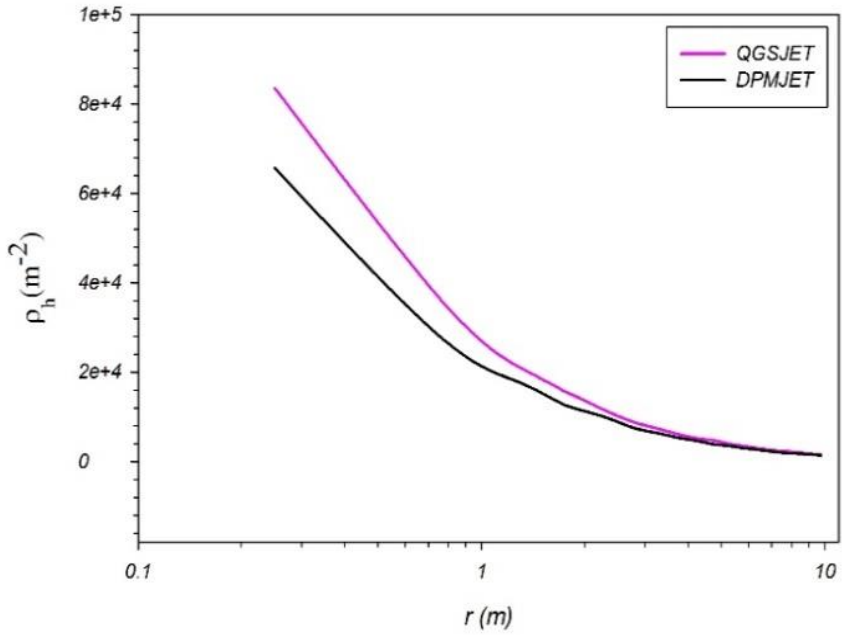


Figure-4. Prediction QGSJET, DPMJET models of lateral distribution of secondary hadrons with primary proton at 10^{19} eV.

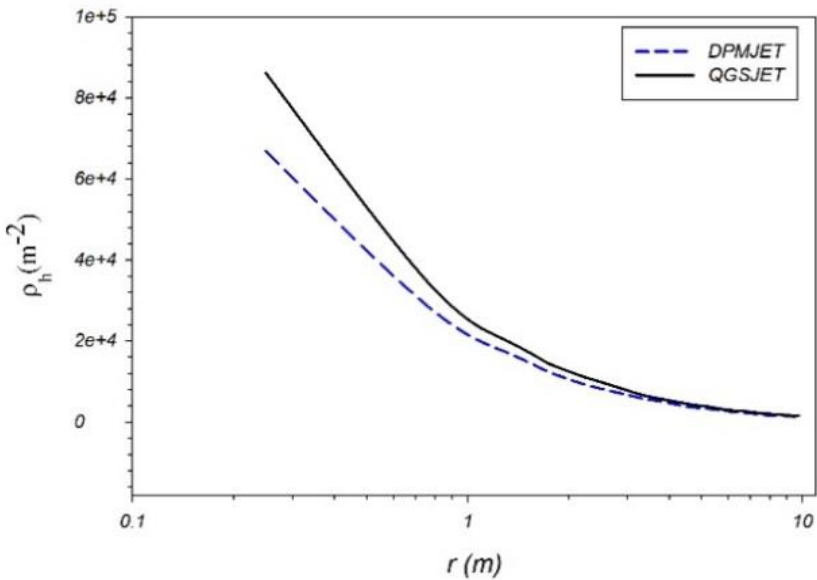


Figure-5. lateral distributions of secondary hadrons for initial proton in the primary energy 10^{19} eV and QGSJET model are fitted with equation 3.

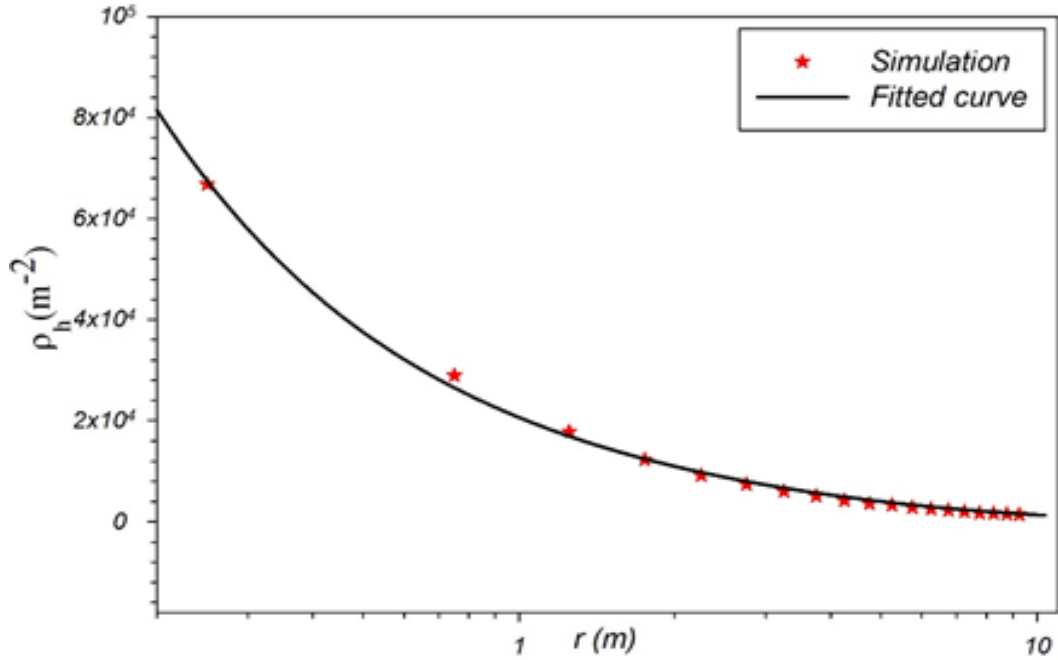


Figure-6. The steepness of lateral distribution of hadrons for primary protons and iron as a function of primary energy with QGSJET model.

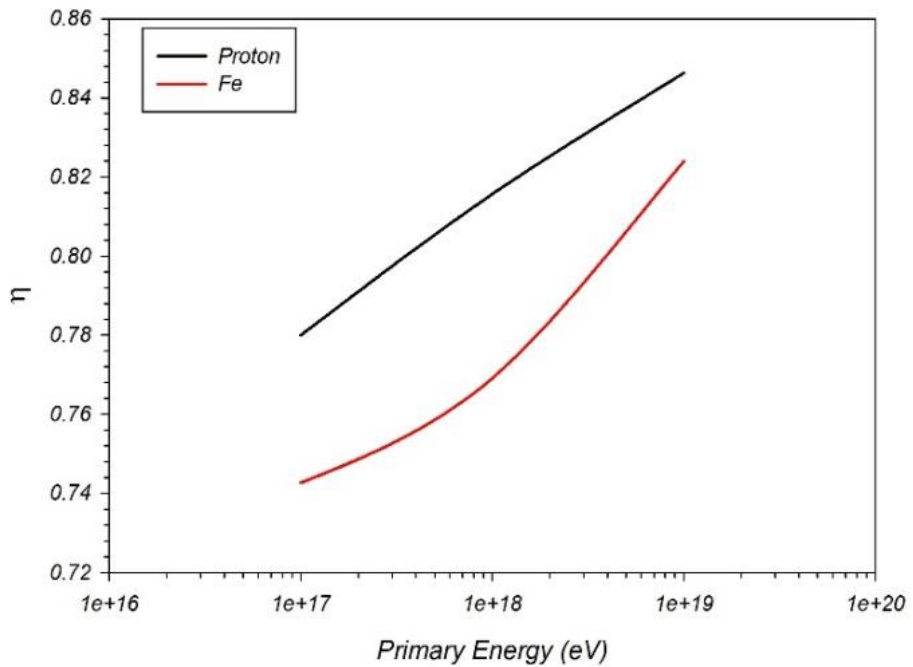


Figure-7. The steepness of lateral distribution of hadrons for primary protons and iron as a function of primary energy with DPMJET model.

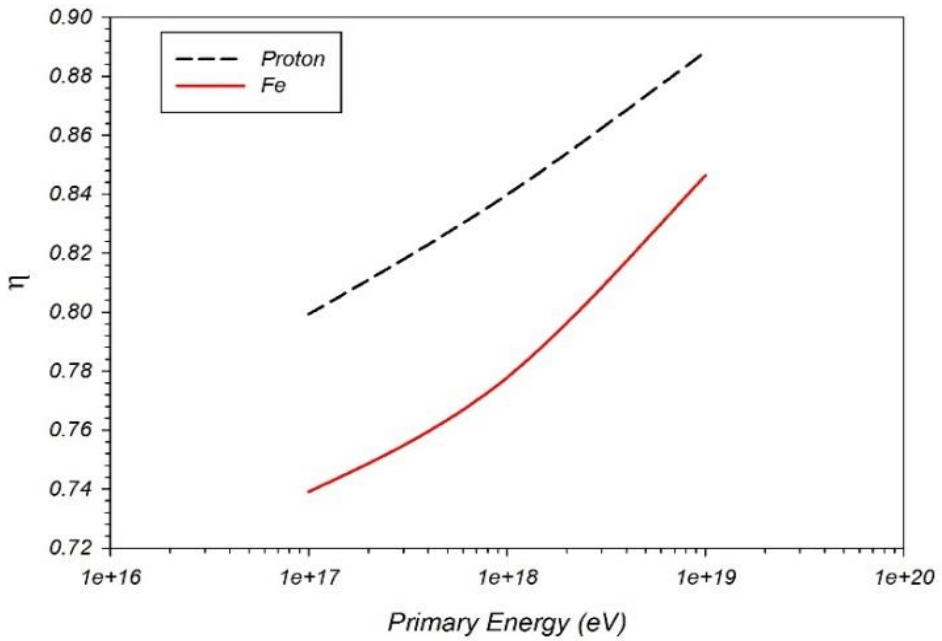


Figure-8. The steepness of hadrons lateral distribution for primary iron as a function of primary energy with DPMJET and QGSJET models.

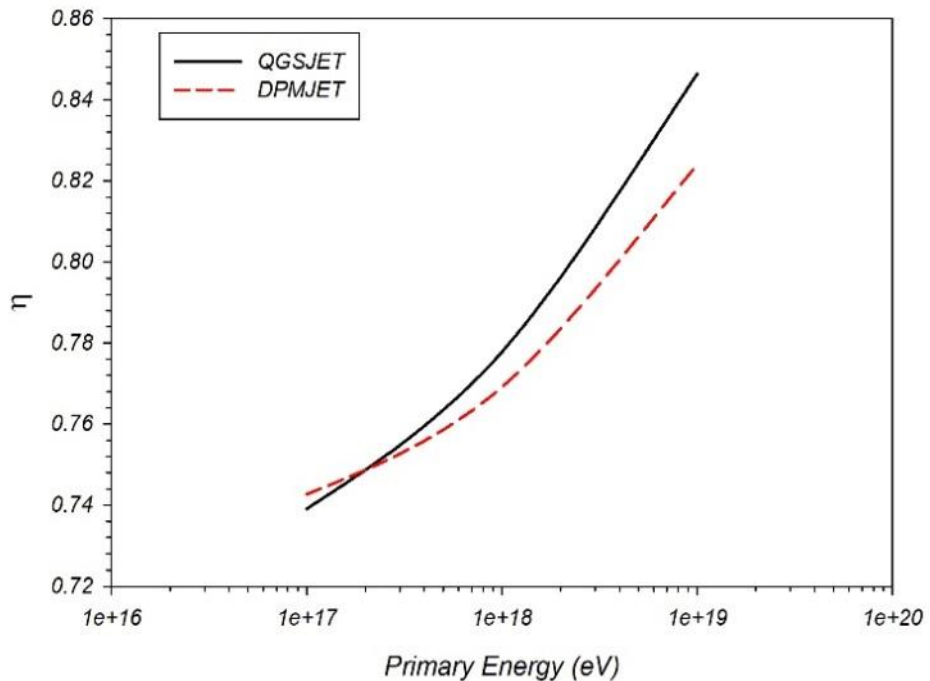


Figure-9. The steepness of lateral distribution of hadrons for primary proton as a function of primary energy with DPMJET and QGSJET models.

